

## Research Article

# Studies on Thermophysical Properties of CaO and MgO by $\gamma$ -Ray Attenuation

A. S. Madhusudhan Rao<sup>1</sup> and K. Narendra<sup>2</sup>

<sup>1</sup> Department of Physics, Varadha Reddy College of Engineering, Warangal 506009, India

<sup>2</sup> Kakatiya University, Warangal 506009, India

Correspondence should be addressed to A. S. Madhusudhan Rao; madhusudhanammiraju@yahoo.com

Received 5 January 2014; Accepted 28 February 2014; Published 15 April 2014

Academic Editor: Mohammad Al-Nimr

Copyright © 2014 A. S. M. Rao and K. Narendra. This is an open access article distributed under the Creative Commons Attribution License, which permits unrestricted use, distribution, and reproduction in any medium, provided the original work is properly cited.

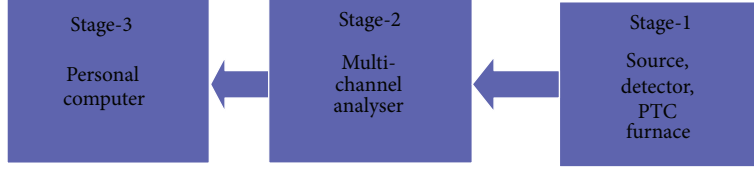
The study on temperature dependent  $\gamma$ -ray attenuation and thermophysical properties of CaO and MgO has been carried out in the temperature range 300 K–1250 K using different energies of  $\gamma$ -beam, namely, Am (0.0595 MeV), Cs (0.66 MeV), and Co (1.173 MeV and 1.332 MeV) on  $\gamma$ -ray densitometer fabricated in our laboratory. The linear attenuation coefficients ( $\mu_l$ ) for the pellets of CaO and MgO as a function of temperature have been determined using  $\gamma$ -beam of different energies. The coefficients of temperature dependence of density have been reported. The variation of density and linear thermal expansion of CaO and MgO in the temperature range of 300 K–1250 K has been studied and compared with the results available in the literature. The temperature dependence of linear attenuation coefficients, density, and thermal expansion has been represented by second degree polynomial. Volume thermal expansion coefficients have been reported.

## 1. Introduction

Density and thermal expansion are fundamental thermophysical properties of solids. The study of temperature dependence of these properties is very important in understanding the temperature variation of other properties like elastic constants, refractive indices, dielectric constants, thermal conductivity, diffusion coefficients, and other heat transfer dimensionless numbers. Thermal expansion of solids is of technical importance as it determines the thermal stability and thermal shock resistance of the material. In general the thermal expansion characteristics decide the choice of material for the construction of metrological instruments and the choice of container material in nuclear fuel technology. A number of methods have evolved for the determination of density and thermal expansion of solids at high temperature like Archimedean method [1–3], pycnometry [4–8], dilatometry [9–12], electromagnetic levitation [13], method of maximal pressure in gas bubble [14–18], method of sessile drop [19], hydrostatic weighing [20, 21], high temperature electrostatic levitation [22], and gamma ray densitometry [23–34]. Using  $\gamma$ -ray attenuation technique Drotning [23]

measured thermal expansion of solid materials at high temperatures. He studied thermal expansion of aluminum and type 303 stainless steel at high temperatures and such studies have been extended by him to study the thermal expansion of metals and glasses in the condensed state [24]. The  $\gamma$ -radiation attenuation technique for the determination of thermophysical properties in the condensed state has several advantages over other methods at high temperatures. This is possible because the  $\gamma$ -ray is not in any kind of physical or thermal contact with the material and hence the thermal losses are also reduced and in addition eliminate sample and probe compatibility problem.

We extended, for the first time, the  $\gamma$ -ray attenuation technique, to carry out the studies on temperature dependence of  $\gamma$ -ray attenuation and thermophysical properties of CaO and MgO. In the present communication, we report the temperature dependence of linear attenuation coefficient for different energies of  $\gamma$ -beam [Am (0.0595 MeV), Cs (0.66 MeV), Co (1.173 MeV and 1.332 MeV)], density, and thermal expansion of CaO and MgO in the temperature range 300 K–1250 K. In order to carry out this work, we have fabricated in our laboratory a  $\gamma$ -ray densitometer and

FIGURE 1: Block diagram of  $\gamma$ -ray densitometer.

a programmable temperature controlled furnace (PTC) which can reach high temperatures. The data obtained in the present work for coefficient of linear thermal expansion of CaO and MgO as a function of temperature have been compared with experimental and theoretical data in the literature. Authors have carried out such studies on different materials like wrought aluminum alloys [29] and alkali halides [30] using the same experimental setup.

## 2. Theory

The technique of  $\gamma$ -ray attenuation method is based on the following fundamental equation:

$$I = I_0 \exp [-\mu \rho l], \quad (1)$$

where  $I_0$  is the intensity of  $\gamma$ -ray before passing through the sample,  $I$  is the intensity of  $\gamma$ -ray after passing through the sample,  $\mu$  is the mass attenuation coefficient of the sample,  $\rho$  is the density of the sample, and  $l$  is the thickness of the sample. It is clear from (1) that any change in the temperature of the solid is accompanied by change in its density causing a change in the measured intensity. The density and thermal expansion of the materials studied in the present work have been determined following the method suggested by Drotning [23]. The relation between coefficient of volumetric thermal expansion ( $\alpha_p$ ) and coefficient of linear thermal expansion ( $\alpha_l$ ) is given by

$$\alpha_p \equiv -3\alpha_l (1 - 2\alpha_l \Delta T), \quad (2)$$

where  $\alpha_p$  and  $\alpha_l$  are mean values over a temperature interval:

$$\Delta T = T_2 - T_1,$$

$$\text{such that } \alpha_l = \frac{(l_2 - l_1)}{(\Delta T) l_1}, \quad \alpha_p = \frac{(\rho_2 - \rho_1)}{(\Delta T) \rho_1}, \quad (3)$$

where  $\rho_1 = \rho(T_1)$ ,  $l_1 = l(T_1)$ , and so forth.

Rewrite (2) as

$$(\Delta T)^2 \alpha_l \alpha_p = z - (\Delta T) \alpha_l - (\Delta T) \alpha_p, \quad (4)$$

where  $z$  is defined by

$$\begin{aligned} z &= \ln \frac{[I(T_1) I_0(T_2) / I(T_2) I_0(T_1)]}{(\mu \rho_1 l_1)} \\ &= \left( \frac{\rho_2 l_2}{\rho_1 l_1} \right) - 1. \end{aligned} \quad (5)$$

Substituting for  $\alpha_p$  from (2) gives

$$\begin{aligned} &- 3(\Delta T)^2 \alpha_l^2 (1 - 2\alpha_l \Delta T) \\ &= z - (\Delta T) \alpha_l + 3(\Delta T) \alpha_l (1 - 2\alpha_l \Delta T), \end{aligned} \quad (6)$$

which can be rewritten as

$$6x^3 + 3x^2 - 2x - z = 0, \quad (7)$$

where

$$x \equiv (\Delta T) \alpha_l. \quad (8)$$

The intensities of  $\gamma$ -radiation with sample  $I$  and without sample  $I_0$  are recorded at every temperature. At room temperature  $T_1$ , thickness of the sample  $l_1$  is measured and using (1)  $\mu$  is determined. Further measurements of  $I$  and  $I_0$  at different temperatures enable the determination of  $z$  by (5) and hence  $x$  can be found from the solution of (7). From the value of  $x$ , mean linear thermal expansion ( $\alpha_l$ ) can be determined as a function of temperature.

## 3. Experimental

The experimental setup used for determination of density of materials utilizing  $\gamma$ -ray attenuation technique is called a  $\gamma$ -ray densitometer. A programmable temperature controlled furnace with sample inside the air tight quartz tube is introduced in the  $\gamma$ -radiation path allowing the beam to pass through the sample and to the detector without any interruption. The temperature of the sample is varied to study the attenuation at various temperatures. The block diagram of  $\gamma$ -ray densitometer used in the present work is shown in Figure 1.

The samples studied in the present work were in the form of pellets. The weight of the powder is 20.0 gm and the thickness of pellet is 1.40 cm with a die set by applying hydraulic press. CaO and MgO pellets were sintered at a temperature of 600 K for densification. The pellet was then firmly mounted on the round sample holder made of flat stainless steel strip inserted into an air tight quartz tube. The sample holder along with the sample was slid through a cork into an air tight quartz tube and was fixed firmly. A diffusion pump was then connected to the sample holder tube for evacuation. For inert atmosphere, argon gas was introduced into the quartz tube through the sample holder tube. Then the quartz tube assembly along with the sample was slid into the programmable temperature controlled (PTC) furnace and fixed at appropriate position ensuring

a perfect alignment of sample with collimation on either side. A programmable temperature controlled furnace with sample inside the air tight quartz tube is introduced in the  $\gamma$ -radiation path allowing the beam to pass through the sample and to the detector without any interruption. The temperature of the sample is varied to study the attenuation at various temperatures. The PTC furnace was programmed in such a way that the furnace temperature is increased by 50 K in every step starting from room temperature and stabilizes there for 5 minutes. Temperature equilibrium is achieved within 5 minutes and temperature accuracy is  $\pm 1\%$  of set point temperature after stabilization. Heating rate between each step of 50 K is 5 K/min. At each temperature the  $\gamma$ -ray counts of photon energies [0.0595 MeV, 0.662 MeV, and 1.173 MeV and 1.332 MeV] emitted by 10 mCi  $^{241}\text{Am}$ , 30 mci  $^{137}\text{Cs}$ , and 11.73  $\mu\text{Ci}$   $^{60}\text{Co}$  radioactive point sources, respectively, with sample ( $I$ ) and without sample ( $I_0$ ) were detected and recorded using a multichannel analyzer. The recording of  $\gamma$ -ray counts was done for a period of 20 minutes at each programmed temperature. After a time of 20 minutes of isothermal holding, the difference of programmed and sample temperature (error) was  $\pm 1\text{ K}$  of set point. Measurement of  $\gamma$ -ray attenuation counts at every step of temperature was repeated before and after the sample was introduced and the average value was considered in all our calculations. The cooling rate varied between 10 K/min from 1300 K to 800 K, 6 K/min from 800 K to 500 K, 4 K/min from 500 K to 400 K, and 2 K/min thereafter up to 300 K. The  $\gamma$ -ray counts were recorded while heating and cooling the sample. This procedure was repeated until the desired temperature range was covered in each case. The gamma radiation detector used in our study is a sodium iodide-thallium activated detector. The 0.0762 m diameter and 0.0762 m thick crystal are integrally coupled to a 0.0762 m diameter photomultiplier tube (PMT). The PMT has a 14-pin base and can be mounted on two types of PMT preamplifier units. The one used in our study is a coaxial in-line preamplifier. The detector has a resolution of 8.5% for 0.662 MeV of  $^{137}\text{Cs}$ .

#### 4. Results and Discussion

The experimentally determined values of mass attenuation coefficients ( $\mu$ ) of CaO and MgO for  $\gamma$ -beam of different energies are compared with the theoretical values obtained from National Institute of Standards and Technology (NIST-X-COM) in Table 1. The results obtained for the temperature dependence of the linear attenuation coefficients ( $\mu_L$ ) of CaO and MgO for  $\gamma$ -beam of different energies are summarized in Table 2. The results obtained for the temperature dependence of the density ( $\rho$ ) and the coefficient of linear thermal expansion ( $\alpha$ ) of CaO and MgO are presented in Table 3. The measurements have been carried out in solid phase only. The experimental data obtained in the present work for the density, the linear attenuation coefficient, and coefficient of linear thermal expansion have been fit to a least squares quadratic polynomial of the following form:

$$\rho(T) = a + bT + cT^2. \quad (9)$$

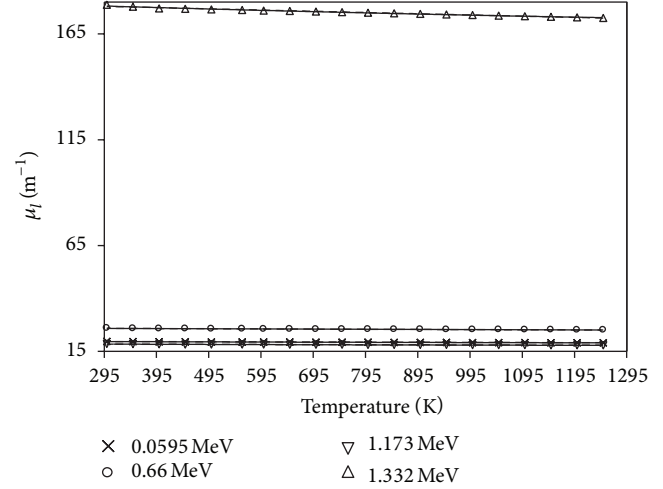


FIGURE 2: Variation of linear attenuation coefficient of CaO with temperature for different  $\gamma$ -sources.

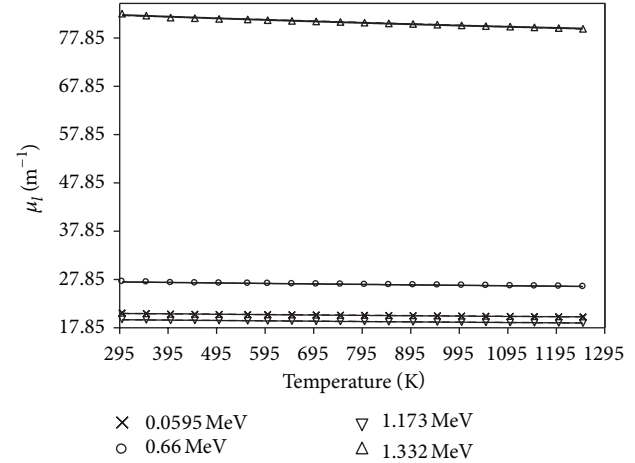


FIGURE 3: Variation of linear attenuation coefficient of MgO with temperature for different  $\gamma$ -sources.

Since the measurements have been made in the limited temperature range the coefficient of volumetric thermal expansion (CVTE) was calculated using the following equation:

$$\beta = \left( \frac{1}{\rho} \right) \left( \frac{d\rho}{dT} \right), \quad (10)$$

where  $(d\rho/dT)$  is the first derivative of density with respect to the absolute temperature which is determined from (9). The variation of linear attenuation coefficients of CaO and MgO with temperature for  $\gamma$ -beam of different energies is shown in Figures 2 and 3, respectively. The variation of density and linear thermal expansion with temperature of CaO and MgO has been shown in Figures 4 and 5, respectively.

**4.1. CaO.** The temperature dependence of linear attenuation coefficient of CaO is a negative linear function of temperature. The temperature dependence of linear attenuation coefficient for different energies of  $\gamma$ -beam [Am (0.0595 MeV),

TABLE 1: Comparison of mass attenuation coefficients ( $\mu$ ) of CaO and MgO of  $\gamma$ -rays with different energies.

$(\mu) 10^{-3} \text{ m}^2 \text{kg}^{-1}$	Cs (0.66 MeV)		Am (0.0595 MeV)		Co (1.173 MeV)		Co (1.332 MeV)	
	NIST X-COM	EXPTL	NIST X-COM	EXPTL	NIST X-COM	EXPTL	NIST X-COM	EXPTL
CaO	7.78	7.76	53.39	53.35	5.89	5.90	5.52	5.52
MgO	7.69	7.67	23.30	23.15	5.84	5.85	5.48	5.47

TABLE 2: Variation of linear attenuation coefficient of CaO and MgO with temperature for different  $\gamma$  energies.

T K	CaO ( $\mu_l \text{ m}^{-1}$ )				MgO ( $\mu_l \text{ m}^{-1}$ )			
	Cs (0.66) MeV	Am (0.0595) MeV	Co (1.173) MeV	Co (1.33) MeV	Cs (0.66) MeV	Am (0.0595) MeV	Co (1.173) MeV	Co (1.33) MeV
300	26.01	178.72	19.73	18.51	27.46	82.88	20.91	19.61
350	25.89	177.87	19.64	18.42	27.33	82.48	20.81	19.51
400	25.76	177.02	19.54	18.32	27.2	82.09	20.71	19.41
450	25.73	176.8	19.52	18.30	27.16	81.95	20.68	19.38
500	25.69	176.54	19.49	18.27	27.11	81.81	20.64	19.35
550	25.66	176.27	19.46	18.24	27.07	81.7	20.61	19.32
600	25.62	176.00	19.43	18.21	27.03	81.56	20.58	19.29
650	25.58	175.79	19.41	18.19	26.99	81.42	20.55	19.26
700	25.54	175.52	19.38	18.16	26.94	81.28	20.51	19.22
750	25.51	175.25	19.35	18.14	26.89	81.16	20.48	19.19
800	25.47	174.99	19.32	18.11	26.84	81.03	20.44	19.16
850	25.43	174.72	19.29	18.08	26.80	80.89	20.41	19.13
900	25.39	174.45	19.26	18.05	26.76	80.75	20.37	19.09
950	25.35	174.19	19.24	18.03	26.72	80.61	20.34	19.06
1000	25.31	173.92	19.21	18.01	26.67	80.47	20.31	19.03
1050	25.27	173.65	19.18	17.98	26.62	80.33	20.27	19.00
1100	25.23	173.39	19.14	17.94	26.57	80.19	20.23	18.96
1150	25.19	173.12	19.11	17.91	26.52	80.05	20.19	18.93
1200	25.15	172.80	19.08	17.88	26.47	79.89	20.15	18.89
1250	25.11	172.53	19.05	17.85	26.42	79.75	20.12	18.86

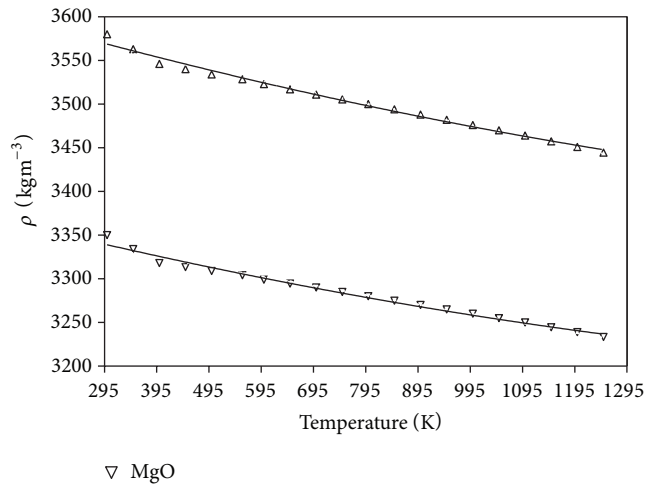


FIGURE 4: Variation of density of CaO and MgO with temperature.

Cs (0.66 MeV), and Co (1.173 MeV and 1.332 MeV)] has been represented by second degree polynomial, respectively:

$$\begin{aligned}
 \mu_l(T) &= (180.49) + (-8.32 \times 10^{-3})T + (1.66 \times 10^{-6})T^2, \\
 \mu_l(T) &= (27.59) + (-1.29 \times 10^{-3})T + (2.60 \times 10^{-7})T^2, \\
 \mu_l(T) &= (19.92) + (-8.90 \times 10^{-4})T + (1.67 \times 10^{-7})T^2, \\
 \mu_l(T) &= (18.70) + (-9.00 \times 10^{-4})T + (1.93 \times 10^{-7})T^2.
 \end{aligned} \quad (11)$$

The density of CaO decreases from a value of  $3350 \text{ kgm}^{-3}$  at 300 K to a value of  $3234 \text{ kgm}^{-3}$  at 1250 K with a decrease of

TABLE 3: Variation of density and coefficient of linear thermal expansion of CaO and MgO with temperature.

T K	CaO		MgO	
	$\rho \text{ kgm}^{-3}$	$\alpha (10^{-6}) \text{ K}^{-1}$	$\rho \text{ kgm}^{-3}$	$\alpha (10^{-6}) \text{ K}^{-1}$
300	3350	11.91	3580	10.42
350	3334	12.01	3563	11.22
400	3318	12.11	3546	12.02
450	3314	12.31	3540	12.47
500	3309	12.51	3534	12.91
559	3304	12.65	3529	13.17
600	3299	12.78	3523	13.42
650	3295	12.93	3517	13.66
700	3290	13.07	3511	13.90
750	3285	13.19	3506	14.10
800	3280	13.31	3500	14.30
850	3275	13.41	3494	14.43
900	3270	13.50	3488	14.55
950	3265	13.62	3482	14.68
1000	3260	13.73	3476	14.81
1050	3255	13.85	3470	14.96
1100	3250	13.97	3464	15.11
1150	3245	14.07	3458	15.28
1200	3239	14.17	3451	15.45
1250	3234	14.29	3445	15.60

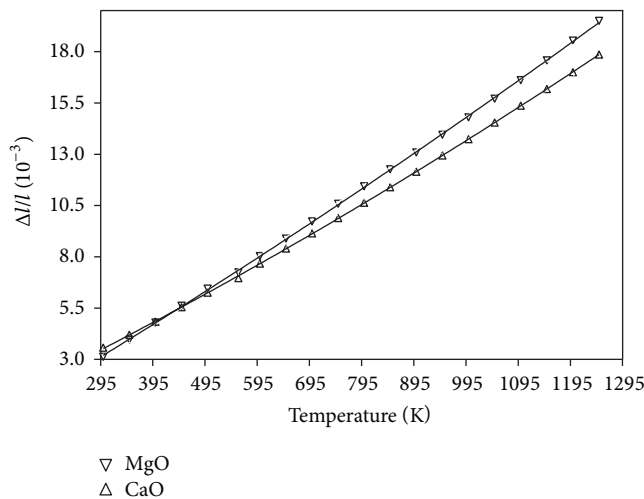


FIGURE 5: Variation of thermal expansion of CaO and MgO with temperature.

about 1.16%. The temperature dependence of density is a negative linear function of temperature. For CaO the temperature dependence of density is represented by quadratic equation:

$$\rho(T) = (3382.77) + (-1.55 \times 10^{-1}) T + (3.04 \times 10^{-5}) T^2. \quad (12)$$

The coefficient of temperature dependence of density is  $-0.122 \text{ kgm}^{-3} \text{ K}^{-1}$  and the coefficient of volume thermal

expansion is  $4.0 \times 10^{-5} \text{ K}^{-1}$  in the temperature range 300 K–1250 K. The thermal expansion increases linearly with temperature and the results on thermal expansion in the temperature range from 300 K to 1250 K have been analyzed by least squares method and are represented by the following polynomial equation:

$$\frac{\Delta l}{l(T)} = (-1.35 \times 10^{-3}) + (1.47 \times 10^{-5}) T + (1.54 \times 10^{-9}) T^2. \quad (13)$$

The coefficient of linear thermal expansion ( $\alpha$ ) of CaO in the temperature range 300 K–1250 K has been represented by second degree polynomial and has been shown in Figure 6 along with data obtained by other methods for comparison:

$$\alpha(T) = (10.84 \times 10^{-6}) + (3.63 \times 10^{-9}) T + (-7.18 \times 10^{-13}) T^2. \quad (14)$$

4.2. *MgO*. The temperature dependence of linear attenuation coefficient of MgO is a negative linear function of temperature. The temperature dependence of linear attenuation coefficient for different energies of  $\gamma$ -beam [Am (0.0595 MeV),

Cs (0.66 MeV), and Co (1.173 MeV and 1.332 MeV)] has been represented by second degree polynomial, respectively:

$$\begin{aligned}\mu_l(T) &= (83.78) + (-4.10 \times 10^{-3})T + (7.46 \times 10^{-7})T^2, \\ \mu_l(T) &= (29.12) + (-1.39 \times 10^{-3})T + (2.39 \times 10^{-7})T^2, \\ \mu_l(T) &= (21.13) + (-1.01 \times 10^{-3})T + (1.68 \times 10^{-7})T^2, \\ \mu_l(T) &= (19.83) + (-9.99 \times 10^{-4})T + (1.89 \times 10^{-7})T^2.\end{aligned}\quad (15)$$

The density of MgO decreases from a value of  $3580 \text{ kgm}^{-3}$  at 300 K to a value of  $3445 \text{ kgm}^{-3}$  at 1250 K with a decrease of about 1.35%. The temperature dependence of density is a negative linear function of temperature. For MgO the temperature dependence of density is represented by the following quadratic equation:

$$\rho(T) = (3619.02) + (-1.77 \times 10^{-1})T + (3.19 \times 10^{-5})T^2. \quad (16)$$

The coefficient of temperature dependence of density is  $-0.142 \text{ kgm}^{-3} \text{ K}^{-1}$  and the coefficient of volume thermal expansion is  $4.0 \times 10^{-5} \text{ K}^{-1}$ . The thermal expansion increases linearly with temperature and the results on thermal expansion in the temperature range from 300 K to 1250 K have been analyzed by least squares method and are represented by the following equation:

$$\begin{aligned}\frac{\Delta l}{l(T)} &= (-2.42 \times 10^{-4}) + (1.20 \times 10^{-5})T \\ &\quad + (2.01 \times 10^{-9})T^2.\end{aligned}\quad (17)$$

The coefficient of linear thermal expansion ( $\alpha$ ) of MgO in the temperature range 300 K–1250 K has been represented by second degree polynomial and has been shown in Figure 7 along with data obtained by other methods for comparison:

$$\begin{aligned}\alpha(T) &= (7.72 \times 10^{-6}) + (0.01 \times 10^{-6})T \\ &\quad + (-4.89 \times 10^{-12})T^2.\end{aligned}\quad (18)$$

The decrease in density in CaO and MgO with temperature can be attributed to the increase in the equilibrium concentration of thermally generated Schottky defects. Another source of generation of defects in CaO and MgO is the irradiation with  $\gamma$ -rays as the technique used in the present study is  $\gamma$ -attenuation technique. However, the values of density seem to have not been affected much by irradiation of  $\gamma$ -rays since the values of coefficient of linear thermal expansion at different temperatures obtained in the present work agree well with data reported in the literature from other methods [35–38] as shown in Figures 6 and 7, respectively. However, the results on variation of density and linear attenuation coefficient of the samples with temperature are not available from other methods for comparison.

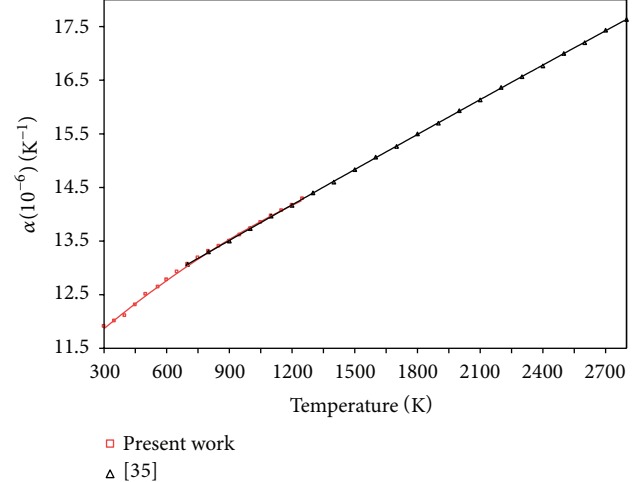


FIGURE 6: Comparison of coefficient of thermal expansion of CaO with data in the literature.

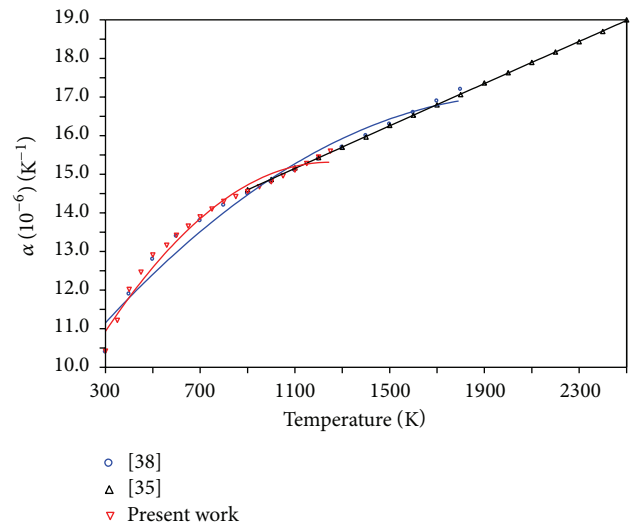


FIGURE 7: Comparison of coefficient of thermal expansion of MgO with data in the literature.

The uncertainty in the measured physical parameters depends on uncertainty in the furnace temperature and measurement of the mass attenuation coefficient, which has been estimated from errors in intensities  $I_0$ ,  $I$  and thickness ( $l$ ) using the following relation [39–41]:

$$\Delta(\mu_m) = \frac{1}{\rho l} \left[ \left( \frac{\Delta I_0}{I} \right)^2 + \left( \frac{\Delta I}{I} \right)^2 + \left( \ln \frac{I_0}{I} \right)^2 + \left( \frac{\Delta l}{l} \right)^2 \right]^{1/2}, \quad (19)$$

where  $\Delta I_0$ ,  $\Delta I$ , and  $\Delta l$  are the errors in the intensities  $I_0$ ,  $I$  and thickness  $l$ , respectively. In this experiment, the intensities  $I_0$  and  $I$  have been recorded for the same time and under the same experimental conditions. Estimated error in these measurements was around 2%.

## 5. Conclusions

The pellets were prepared with fine powder of CaO and MgO with a diameter of 20 mm with varying thicknesses with a die set by applying hydraulic press. The  $\gamma$ -ray attenuation measurements of CaO and MgO have been made using  $\gamma$ -beam of different energy sources on a  $\gamma$ -ray densitometer. The results on the variation of density and linear thermal expansion with temperature of both the pellets are found to be equal for all the  $\gamma$ -energy sources. The results on the variation of linear attenuation coefficient, density, and linear thermal expansion with temperature of these pellets have been reported and these variations have been represented by quadratic equations. The results on these pellets by using  $\gamma$ -ray attenuation technique are being reported for the first time.

## Conflict of Interests

The authors hereby declare that there is no issue of any type of conflict of interests in any manner.

## Acknowledgment

The authors thank University Grants Commission (UGC), New Delhi, for the financial assistance through Special Assistance Programme (SAP) no. F.530/8/DRS/2009 (SAP-1).

## References

- [1] B. B. Alchagirov and A. M. Chochaeva, "Temperature dependence of the density of liquid tin," *High Temperature*, vol. 38, no. 1, pp. 44–48, 2000.
- [2] L. Wang, Q. Wang, A. Xian, and K. Lu, "Precise measurement of the densities of liquid Bi, Sn, Pb and Sb," *Journal of Physics: Condensed Matter*, vol. 15, no. 6, pp. 777–783, 2003.
- [3] X. Chen, Q. Wang, and K. Lu, "Temperature and time dependence of the density of molten indium antimonide measured by an improved archimedean method," *Journal of Physics: Condensed Matter*, vol. 11, no. 50, pp. 10335–10341, 1999.
- [4] B. B. Alchagirov, A. G. Mozgovoy, T. M. Taova, and T. A. Sizhahzev, *Advanced Materials*, vol. 6, no. 35, 2005.
- [5] B. B. Alchagirov, T. M. Shamparov, and A. G. Mozgovoy, "Experimental investigation of the density of molten lead-bismuth eutectic," *High Temperature*, vol. 41, no. 2, pp. 210–215, 2003.
- [6] A. F. Crawley, "Densities and viscosities of some liquid alloys of zinc and cadmium," *Metallurgical Transactions B*, vol. 3, no. 4, pp. 971–975, 1972.
- [7] K. Mukai, F. Xiao, K. Nogi, and Z. Li, "Measurement of the density of Ni-Cr alloy by a modified pycnometric method," *Materials Transactions*, vol. 45, no. 7, pp. 2357–2363, 2004.
- [8] Y. Sato, T. Nishizuka, K. Hara, T. Yamamura, and Y. Waseda, "Density measurement of molten silicon by a pycnometric method," *International Journal of Thermophysics*, vol. 21, no. 6, pp. 1463–1471, 2000.
- [9] U. Jauch, G. Hasse, and B. Schulz, "Part 11: thermophysical properties of Li(17)Pb(83) eutectic alloy," in *Thermophysical Properties in the System Li-Pb*, vol. 25, Kernforschungszentrum Karlsruhe, Karlsruhe, Germany, 1986.
- [10] L. Wang and Q. Mei, "Density measurement of liquid metals using dilatometer," *Journal of Materials Science & Technology*, vol. 22, no. 4, pp. 569–571, 2006.
- [11] G. K. White and J. G. Collins, "The thermal expansion of alkali halides at low temperatures. II. Sodium, rubidium and caesium halides," *Proceedings of the Royal Society A: Mathematical, Physical & Engineering Sciences*, vol. 333, pp. 237–259, 1973.
- [12] "Pb-free solders and other materials," *Journal of Electronic Materials*, 2011.
- [13] J. Brillo, I. Egry, and I. Ho, "Density and thermal expansion of liquid Ag-Cu and Ag-Au alloys," *International Journal of Thermophysics*, vol. 27, no. 2, pp. 494–506, 2006.
- [14] S. A. Been, H. S. Edwards, C. E. Tector, and V. P. Calkins, "ORNL: fairchild and airplane corporation," NEPA Report 1585, 1950.
- [15] Fairchild Engine and Airplane Corporation, Oak Ridge, Tenn, USA.
- [16] H. Ruppertsberg and W. Speicher, "Density and compressibility of liquid Li-Pb alloys," *Zeitschrift Naturforschung Teil A*, vol. 31, pp. 47–52, 1976.
- [17] J. Saar and H. Ruppertsberg, "Calculation of  $C_p(T)$  for liquid Li/Pb alloys from experimental  $\rho(T)$  and  $(\delta\rho/\delta T)_s$  data," *Journal of Physics F: Metal Physics*, vol. 17, no. 2, pp. 305–314, 1987.
- [18] F. T. Firdu and P. Taskinen, *Aalto University Publications in Material Science and Engineering*, Espoo TKK-MT-215, 2010.
- [19] I. V. Kazakova, S. A. Lyamkyn, and B. M. Lepinskikh, *The Journal of Physical Chemistry*, vol. 58, p. 1534, 1984.
- [20] N. A. Nikol'skyi, N. A. Kalakutskaya, I. M. Pehelkin, T. V. Klassen, and V. A. Vel'mishcheva, "Teploenergetika (Power Engineering)," vol. 2, no. 92, 1959.
- [21] N. A. Nikol'skyi, N. A. Kalakutskaya, I. M. Pehelkin, T. V. Klassen, and V. A. Vel'mishcheva, "Voprosy teploobmena," *Problems of Heat Transfer*.
- [22] S. K. Chung, D. B. Thiessen, and W.-K. Rhim, "A noncontact measurement technique for the density and thermal expansion coefficient of solid and liquid materials," *Review of Scientific Instruments*, vol. 67, no. 9, pp. 3175–3181, 1996.
- [23] W. D. Drotning, "Thermal expansion of solids at high temperatures by the gamma attenuation technique," *Review of Scientific Instruments*, vol. 50, no. 12, Article ID 121567, pp. 1567–1570, 1979.
- [24] W. D. Drotning, "Thermal expansion of the group IIb liquid metals zinc, cadmium and mercury," *Journal of The Less-Common Metals*, vol. 96, pp. 223–227, 1984.
- [25] W. D. Drotning, "Thermal expansion of iron, cobalt, nickel, and copper at temperatures up to 600 K above melting," *High Temperatures-High Pressures*, vol. 13, no. 4, pp. 441–458, 1981.
- [26] G. M. Kalinin et al., "Study of Li<sub>17</sub>-Pb<sub>83</sub> eutectic properties," *USSR Contribution to ITER*. In press.
- [27] R. A. Khairulin, A. S. Kosheleva, and S. V. Stankus, "Thermal properties of liquid alloys of magnesium-lead system," *Thermophysics and Aeromechanics*, vol. 14, no. 1, pp. 75–80, 2007.
- [28] R. A. Khairulin, S. V. Stankus, R. N. Abdullaev, Y. A. Plevachuk, and K. Y. Shunyaev, "The density and the binary diffusion coefficients of silver-tin melts," *Thermophysics and Aeromechanics*, vol. 17, no. 3, pp. 391–396, 2010.
- [29] K. Narendar, A. S. M. Rao, K. G. K. Rao, and N. G. Krishna, "Thermo physical properties of wrought aluminum alloys 6061, 2219 and 2014 by gamma ray attenuation method," *Thermochimica Acta*, vol. 569, pp. 90–96, 2013.

- [30] A. S. M. Rao, K. Narender, K. G. K. Rao, and N. G. Krishna, "Thermophysical properties of rubidium and lithium halides by gamma ray attenuation technique," *High Temperature*. In press.
- [31] S. V. Stankus, R. A. Khairulin, A. G. Mozgovoy, V. V. Roshchupkin, and M. A. Pokrasin, "The density and thermal expansion of eutectic alloys of lead with bismuth and lithium in condensed state," *Journal of Physics: Conference Series*, vol. 98, no. 6, Article ID 062017, 2008.
- [32] S. V. Stankus and P. V. Tyagel'skii, "Density of high-purity dysprosium in the solid and liquid states," *High Temperature*, vol. 38, no. 4, pp. 555–559, 2000.
- [33] S. V. Stankus, R. A. Khairulin, A. G. Mozgovoi, V. V. Roshchupkin, and M. A. Pokrasin, "An experimental investigation of the density of bismuth in the condensed state in a wide temperature range," *High Temperature*, vol. 43, no. 3, pp. 368–378, 2005.
- [34] S. V. Stankus, R. A. Khairulin, and A. G. Mozgovoi, "Experimental study of density and thermal expansion of the advanced materials and heat transfer agents for liquid metal systems of thermonuclear reactor: lithium," *High Temperature*, vol. 49, no. 2, pp. 187–192, 2011.
- [35] S. K. Srivastava, P. Sinha, and M. Panwar, "Thermal expansivity and isothermal bulk modulus of ionic materials at high temperatures," *Indian Journal of Pure & Applied Physics*, vol. 47, no. 3, pp. 175–179, 2009.
- [36] K. Y. Singh and B. R. K. Gupta, "A simple approach to analyse the thermal expansion in minerals under the effect of high temperature," *Physica B: Condensed Matter*, vol. 334, no. 3-4, pp. 266–271, 2003.
- [37] B. P. Singh, H. Chandra, R. Shyam, and A. Singh, "Analysis of volume expansion data for periclase, lime, corundum and spinel at high temperatures," *Bulletin of Materials Science*, vol. 35, no. 4, pp. 631–637, 2012.
- [38] R. E. Taylor, *Thermal Expansion of Solids*, ASM International, Materials Park, Ohio, USA, 1998.
- [39] I. Han and L. Demir, "Studies on effective atomic numbers, electron densities and mass attenuation coefficients in Au alloys," *Journal of X-Ray Science and Technology*, vol. 18, no. 1, pp. 39–46, 2010.
- [40] D. Demir, A. Turşucu, and T. Öznülür, "Studies on mass attenuation coefficient, effective atomic number and electron density of some vitamins," *Radiation and Environmental Biophysics*, vol. 51, no. 4, pp. 469–475, 2012.
- [41] N. Kucuk, Z. Tumsavas, and M. Cakir, "Determining photon energy absorption parameters for different soil samples," *Journal of Radiation Research*, vol. 54, no. 3, pp. 578–586, 2013.

